



Research on reservoir characteristics of Chang7 tight oil based on nano-CT

Lei Song¹ · Zhengfu Ning¹ · Lian Duan¹

Received: 22 December 2017 / Accepted: 16 August 2018 / Published online: 25 August 2018
© Saudi Society for Geosciences 2018

Abstract

The microstructure characteristics of the reservoir are closely related to the seepage capacity of the reservoir. Compared with conventional reservoirs and low permeability reservoirs, the tight oil is stored in a smaller nanoporous space. The microscopic pore structure of reservoir is the geometrical shape, size, distribution, and interconnected relationship of porosity and throat. The experiment was conducted on several tight rock samples taken from the Chang 7 formation in Xunyi county of Ordos Basin, China. Based on nano-CT scanning and advanced image processing technology Avizo, we build a three-dimensional comprehensive pore and throat network model. In the result of our study, reservoir space types are dissolution pores with mineral particles inside in the pore network model. Then, the pore throat morphology in the forms of small globular and tubular with SEM was explained. There is a big difference in quantity distribution at different locations, which is limited to the permeability of samples. Pore types are mostly round tubular and long tubular, while isolated pores account for a significant proportion. Through making and analyzing the three-dimensional structure of interconnected pores, obtained their specific forms and the division of connectivity types.

Keywords Tight oil reservoir · Nano-CT scanning · Pore structure · Pore microcosmic morphology

PACS 61.05.–a61.43.Bn81.70.Cv81.16.Rf

Introduction

In recent years, influenced by increasing demand of global energy, unconventional reservoir has become a new hotspot in the past decade due to its enormous exploration potential. Tight oil (such as Bakken oil in Williston basin, North America) and Eagle Ford oil (South Texas, USA) had been exploited commercially with the successful application of horizontal drilling and multistage hydraulic fracturing technology. Tight oil reservoir has become the focus of research in global petroleum geology. Tight sandstones and shale stored a considerable amount of hydrocarbon in their pore networks (Liu et al. 2016; Butcher and Lemmens 2011; Didar and

Akkutlu 2013). Only by understanding the structure of reservoir can make more accurate predictions of tight oil (Kou et al. 2016). Contrast to conventional hydrocarbon resources, the pore structure of tight reservoirs was difficult to characterize because of the ultra-fine pore throat (Clarkson et al. 2012). Reservoir structure affects water flooding development (Hadia et al. 2012), and reservoir structure has an important impact on the final development of tight oil reservoirs (Desbois et al. 2011; Slatt and O'Brien 2011).

Currently, there are three kinds of methods for characterizing reservoirs in the world. The first category is indirect measurement, which includes the common mercury porosimetry (include pressure-controlled porosimetry and rate-controlled porosimetry), gas adsorption method, semi-permeable bulk-head method, centrifuge method, dynamic displacement method, and vapor pressure method. Indirect method has the advantage of large sample size and the results are easy to quantify; the disadvantage is not intuitive, the results are not easy to verify, and the influence of heterogeneity is large in the microscopic scale. The second method is a direct observation method, which includes casting thin section method, image analysis method, various fluorescence agent injection methods, and focusing electron-ion double beam scanning

This article is part of the Topical Collection on *Geo-Resources-Earth-Environmental Sciences*

✉ Lei Song
songleizsy@163.com

¹ School of Petroleum Engineering, China University of Petroleum, Beijing, China

Table 1 Basic data of samples

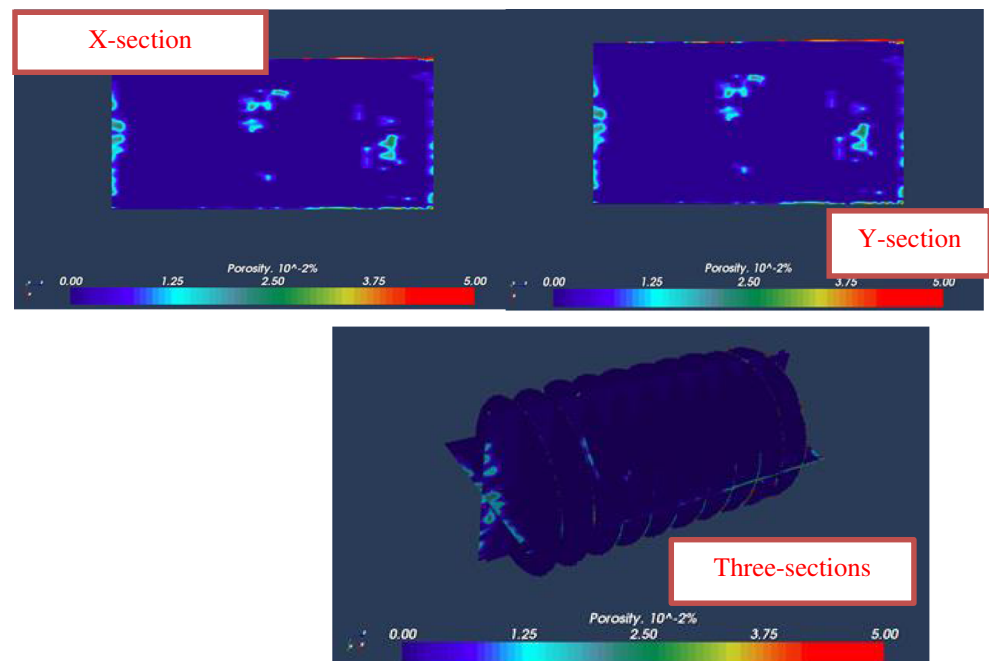
Sample No.	Lithological description	Clay mineral content (%)	Brittle mineral content (quartz + calcite, %)	Feldspar content (%)	Gas permeability (mD)	Porosity (%)
A	Dark-gray mudstone mixed with siltstone	30.2	42.5	22.9	0.19	10.1
B	Dark-gray siltstone	10.5	59.9	19.8	0.22	10.8

electron microscopy (FIB-SEM). The advantages of this method are intuitionistic, accurate, and few influencing factors (Le et al. 2014; Tekin et al. 2014; Xiangjun et al. 2014). The disadvantages are that the scale is small and the resolution is limited. The third method is digital core method with CT, which includes casting model method and digital core pore structure three-dimensional model reconstruction technology. This method can characterize the three-dimensional pore structure and use the three-dimensional digital core to qualitatively explain the pore throat size, connectivity, and morphology (Djendel et al. 2014; Dal Ferro et al. 2011; Boran et al. 2014; Tariq et al. 2010). At present, many scholars have used this experimental means to the microstructure and characteristics of the material (Koru and Serçe 2014; Altan et al. 2014). For the mercury intrusion experiment and scanning electron microscopy experimental analysis method, CT has the advantage of rock samples omnidirectional, large-scale rapid nondestructive scanning imaging. The digital core obtained by CT scan can study the microscopic pore characteristics of the reservoir more intuitively, and its application in the evaluation direction of micro pore structure will be more extensive. In the research of predecessors, such as Qu Le and H.O. Tekin, the CT scan of conventional reservoirs is carried

out, and the characterization is carried out on the micro scale or larger scale. Scholars often use a single research method such as scholar Liu Xiangjun. In this paper, we use the advanced nano-CT test method to establish the Chang 7 tight reservoir in the Ordos Basin from two-dimensional slice to three-dimensional model and characterize the pore structure of China's important tight reservoirs at the nano meter level. The scanning was numerically explained by Avizo software. The three-dimensional pore type and connectivity were identified by nano-CT combined with SEM.

Experimental samples

These experimental samples are from the field outcrop of the Chang 7 reservoir, which located at the Xunyi area, Ordos Basin, China. The Chang 7 oil group is the major production layer of Mesozoic; sandstone is the major tight oil reservoir, with the thickness of 100–125 m. The types of reservoir rocks are mainly fine-grained feldspar-porphry sandstone and feldspar lithic sandstones. The quartz content is relatively high and the feldspar content is low, but the dissolution is common in this region, which results in the development of secondary

Fig. 1 XYZ three directions scan display

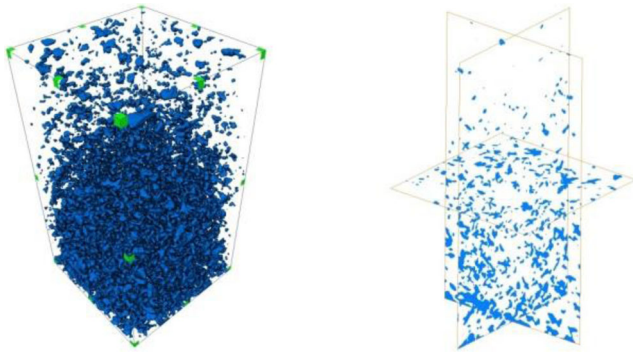


Fig. 2 a, b 3D view and slice view of the distribution of pores

pores. The average porosity is 10.1% and the average air permeability is 0.18 mD. The lithology is characterized by dark-gray mudstone mixed with siltstone, gray-black oil shale, and gray-green siltstone-fine sandstone partially mixed with muddy siltstone, dark-gray mudstone, and gray-black oil shale. Measured through experiments, the basic data are showed in the Table 1.

Characteristics of tight reservoir based on nano-CT

In this study, the collection of the three-dimensional images is completed by the NANO-CT-400 produced from the US Xradia company, whose maximum sampling resolution could account to 1 nm. The experimental sample is a cylindrical sandstone with a diameter of 8 mm. One sample can obtain 983 two-dimensional CT slices of 980×1005 pixels with a

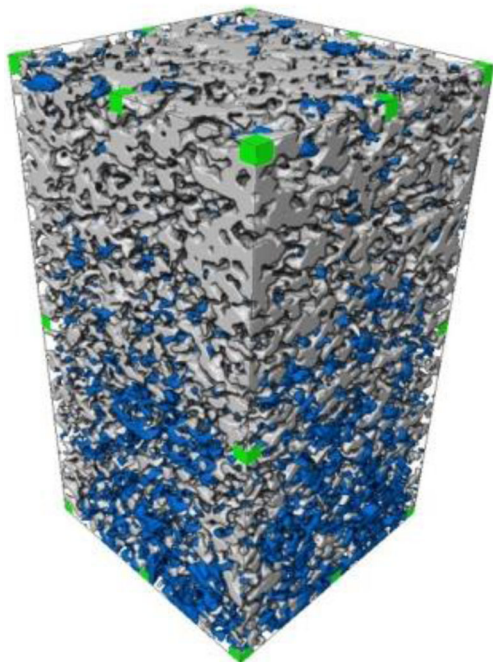


Fig. 3 3D composite view of the distribution of mineral phase and pores

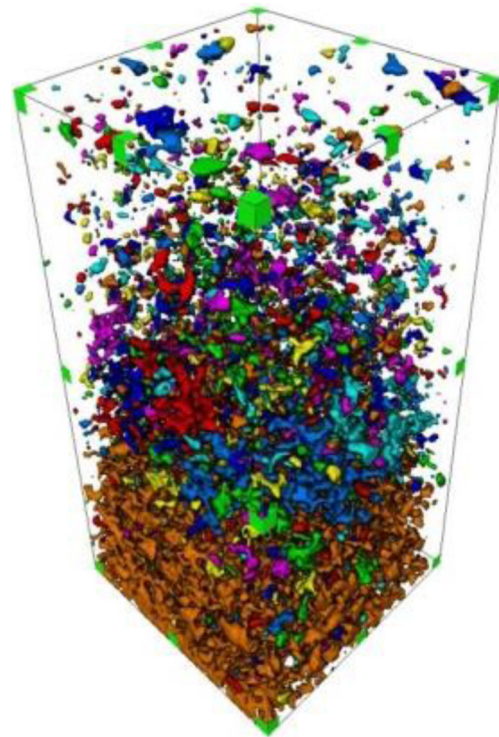


Fig. 4 3D reconstruction image of different types of connected pores in tight core at micron scale

spatial resolution of $2.1 \mu\text{m}/\text{voxel}$, and these two-dimensional slices are in turn to obtain the rock dimensional gray scale image. Gray scale plots, gray, white rock skeletons (high density), and black pore (low density) are clearly visible in the image. All the samples were at the same experimental conditions, that is, the test temperature was $20 \text{ }^\circ\text{C}$ and the single exposure time was 120 s. The total scan time was 54 h.

The porosity of the core surface in Fig. 1 is shown in highlight color, and the three-dimensional model of the core is formed by two-dimensional scanning of three-dimensional x , y , and z directions, and finally stacking the two-dimensional sections in sequence.

Construction of 3D pore structure

The representative elementary volume (REV) was extracted from the original 3D micro-CT images, which can represent the microstructure of the pore and various petro physical properties. It can also avoid the excessive demands on the computer processing capacity. The threshold data based on 2D slice images can be processed by digital segmentation on the REV of 3D micro-CT images to decide what the pore is and what is not. The Marching Cube algorithm was used to extract the surface triangles of the digital images and fit the subsurface to produce estimates of the distribution of pore in the REV. The distribution of pore is shown in Fig. 2a, and the slices of pore are shown in Fig. 2b.

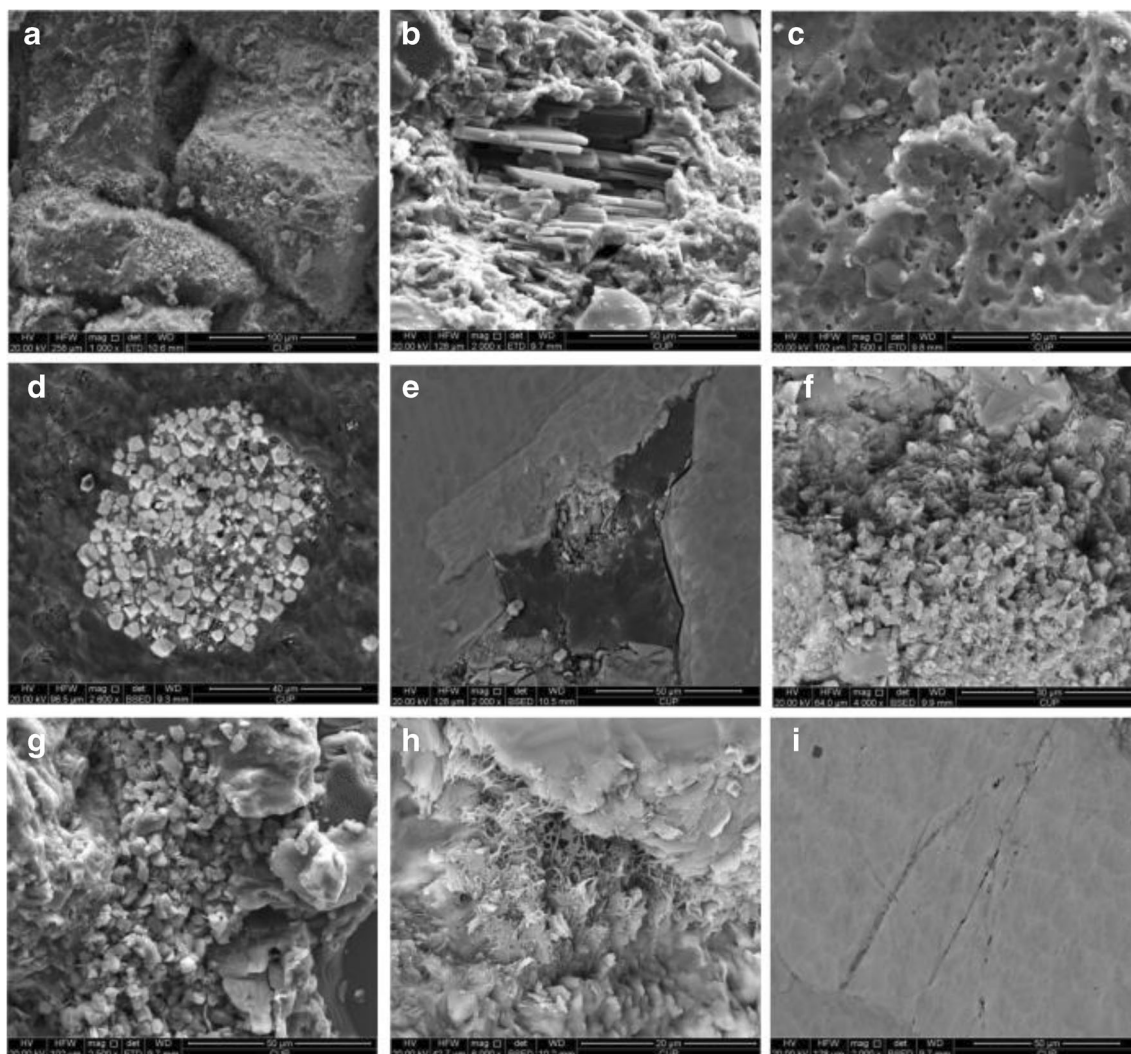


Fig. 5 Pore types in tight sandstones. **a** Residual intergranular pore, chlorite envelope. **b** Skeleton mineral dissolution pores, feldspar. **c** Skeleton mineral dissolution pores, calcite. **d** Pyrite intergranular hole. **e**

Organic hole. **f** Clay mineral crystal hole, kaolinite, chlorite. **g** Clay mineral crystal hole, kaolinite. **h** Clay mineral crystal hole, illite. **i** Micro fractures, mineral backbone cleavage seam

The 3D distribution of minerals is determined by digitally segmenting the REV based on the threshold date when selecting the mineral components in the 2D slice image. The 3D composite view of the distribution of mineral phase and pore is extracted (Fig. 3). It can be seen from the figure that the mineral phase accumulates at one end of the sample, and the content of mineral phase is high, where the pore type is poor.

Connectivity analysis

The 3D distribution pattern of different types of connected pores based on the above steps is showed in Fig. 4. Different colors indicate different connected pores, the same color indicates the same connected pores; the skeleton (quartz) does not show.

Through analyzing the porosity connectivity, the multi-scale and multi-type porosity and pore micro-distribution of

reservoirs show severe heterogeneity. The proportion of isolated pores occupies a large proportion. The source of these isolated pores mainly includes two aspects: one is the isolated pores existing in the core sample, which accounts for the main reason; the other is that in the process of threshold segmentation, the pores separate into isolated pores due to improper selection of threshold value; this part of the proportion is smaller. The visible pore volume fraction is little, and its type dominated by intergranular residual and feldspar pores. The pore shapes are mostly tubular and long tubular, and the connection between the pores is complex. Quantitative analysis shows that the percentage of micron porosity is more than 93%, which is the main storage space of tight oil. The effective configuration of pore throat structure is the main determinants of reservoir permeability, and some of the throats are large and the connectivity is good, which provides a good channel for tight oil migration in reservoir.

SEM analysis

The results of SEM showed that the types of tight reservoir pore include residual intergranular pore, corrosion hole, pyrite intergranular pore, organic hole, and clay minerals holes. Residual intergranular pore is usually associated with quartz, feldspar, and other mineral skeleton, which shows green clay film in common, but occasionally emerges in secondary quartz (Fig. 5a). Their distribution is dispersed in the reservoir, and they are larger pores whose size is between 64 and 600 μm with irregular shape. Dissolution pores are usually in the feldspar type, occasionally in quartz or calcite dissolved pore (Fig. 5b, c); a small amount of feldspar dissolved pore can form a mold hole with pore size of tens of microns. Pyrite ball is commonly seen in tight oil reservoirs, and intergranular pore is mostly triangular with smaller aperture (Fig. 5d). The presence of organic indicates the reservoirs are near the source since the organic is still in the oil window; thus, pores are not developed, and whose size is usually around tens of nanometers (Fig. 5e). In tight oil reservoirs, clay content is high, accounting for 18.21% of the mineral content in various shapes (Fig. 5f–h); thus, there is a large difference on clay mineral hole aperture. Most natural fractures are curved, whose crack width is between 68 and 1.34 μm , and extension length from a few microns to tens of microns. And they often associate with other cracks (Fig. 5i).

SEM results can be used to analyze the causes of tight oil reservoir characteristics. Between 80 and 500 μm corresponds to the type of residual intergranular pore hole. Pore radius between 1 and 10 μm corresponds to pore type of dissolution holes and some of the larger clay mineral holes. With radius of less than 1 μm , pores have complex composition, including dissolution hole, hole clay minerals, and micro-cracks. There are some differences in pore size range of different types of pores, and all kinds of pore development situation of different samples are not the same, which leads to multimodal form in the part of the nanoscale pore radius of distribution curve. There are no preferred pore types corresponding to pores radius between 10 and 80 μm ; thus, it accounted small pore volume ratio.

Conclusion

1. Using the technology of nano-CT scanning and three-dimensional reconstruction can characterize pore and throat structure in tight oil reservoir, which can help us understand its shape, size, connectivity, and spatial distribution characteristics clearly and comprehensively.
2. Each mineral composition and microscopic pore distribution presents serious microscopic heterogeneity in tight oil reservoirs within the micron scale. Pore types are mostly intergranular and dissolution pores; pore shapes are

mostly round tubular and long tubular, while isolated pores account for a significant proportion.

3. With SEM analysis, intergranular pores, corrosion hole, pyrite intergranular pore, organic hole, clay minerals holes, etc. are present in tight oil reservoir of Chang 7 reservoir, China.

Acknowledgements The authors would like to express their sincere thanks to the National Natural Science Fund of China (No.51474222) for permission to publish the results of this study.

Funding information This study received financial support from National Natural Science Fund of China (No. 51474222).

References

- Altan H, Bilgic F et al (2014) Nanomechanical Properties of different dental restorative materials. International Conference on Computational and Experimental Science and Engineering (ICCESEN 2014), Antalya-Turkey. <https://doi.org/10.12693/APhysPolA.130.394>
- Boran F, Çetinkaya S, Şahin M (2014) Effect of surfactant types on the size of tin oxide nanoparticles. International Conference on Computational and Experimental Science and Engineering (ICCESEN 2014), Antalya-Turkey. <https://doi.org/10.12693/APhysPolA.132.546>
- Butcher AR, Lemmens HJ (2011) Advanced SEM technology clarifies nanoscale properties of gas accumulations in shales. Am. Oil Gas Report
- Clarkson CR et al (2012) Characterization of tight gas reservoir pore structure using USANS/SANS and gas adsorption analysis. Fuel 95:371–385. <https://doi.org/10.1016/j.fuel.2011.12.010>
- Dal Ferro N, Delmas PC et al (2011) Coupling X-ray microtomography and mercury intrusion porosimetry to quantify aggregate structures of a cambisol under different fertilisation treatments. Soil Tillage Res 119:13–21. <https://doi.org/10.1016/j.still.2011.12.001>
- Desbois G, Urai JL, Kukla PA et al (2011) High-resolution 3D fabric and porosity model in a tight gas sandstone reservoir: a new approach to investigate microstructures from mm-to nm-scale combining argon beam cross-sectioning and SEM imaging. J Pet Sci Eng 78:243–257. <https://doi.org/10.1016/j.petrol.2011.06.004>
- Didar, B. R. & Akkutlu, I. Y. (2013) Pore-size dependence of fluid phase behavior and properties in organic-rich shale reservoirs. In SPE International Symposium on Oilfield Chemistry. Society of Petroleum Engineers, Texas, USA
- Djendel M, Allaoui O, Boubaaya R (2014) Characterization of alumina-titania coatings produced by atmospheric plasma spraying on 304 SS Steel. International Conference on Computational and Experimental Science and Engineering (ICCESEN 2014, Antalya-Turkey. <https://doi.org/10.12693/APhysPolA.132.538>
- Hadia NJ, Hansen T, TweheyoMT TO (2012) Influence of crude oil components on recovery by high and low salinity waterflooding. Energy Fuels 26:4328–4335. <https://doi.org/10.1021/ef3003119>
- Koru M, Serçe O (2014) Experimental and numerical determination of casting-mold interfacial heat transfer coefficient in the high pressure die casting of A-360 Aluminum. International Conference on Computational and Experimental Science and Engineering (ICCESEN 2014), Antalya-Turkey. <https://doi.org/10.12693/APhysPolA.130.453>
- Kou R., Alafnan S. F. K. & Akkutlu I. Y (2016) Coupling of Darcy's equation with molecular transport and its application to upscaling

- kerogen permeability. SPE Europec featured at 78th EAGE Conference and Exhibition, Vienna, Austria
- Le Q, Wei S, Huaihong D et al (2014) Characterization and application of 3 D digital core pore structure based on CT scanning: a case study of Sangonghe Formation in Well 116 of Mo North Oilfield. *Mod Geol* 28:190–196
- Liu Y, Liu H et al (2016) Quantitative Characterization of dynamic heterogeneity in reservoirs with stratified noncommunicating layers. *J Energy Resour Technol* 139:012901–0129011. <https://doi.org/10.1115/1.4033624>
- Slatt RM, O'Brien NR (2011) Pore types in the Barnett and Woodford gas shales: contribution to understanding gas storage and migration pathways in fine-grained rocks. *AAPG Bull* 95:2017–2030
- Tariq F, Haswell R, Lee PD, McComb DW (2010) Characterization of hierarchical pore structures in ceramics using multiscale tomography. *Acta Mater* 59:2109–2120. <https://doi.org/10.1016/j.actamat.2010.12.012>
- Tekin HO, Altunsoy EE, Manici T, Yilmaz B (2014) Quantitative characteristic X-ray analysis for different compound samples by using Monte Carlo method. International Conference on Computational and Experimental Science and Engineering (ICCESEN 2014), Antalya-Turkey. <https://doi.org/10.12693/APhysPoLA.132.439>
- Xiangjun L, Zhu H, Liang L (2014) Digital petrophysical experiment of sandstone based on micro-CT technology. *Chin J Geophys* 57: 1133–1140. <https://doi.org/10.6038/cjg20140411>